



Antisense locked nucleic acid gapmers to control *Candida albicans* filamentation

Daniela Araújo, PhD^a, Dalila Mil-Homens, PhD^b, Maria Elisa Rodrigues, PhD^a,
Mariana Henriques, PhD^a, Per Trolle Jørgensen, MSc^c, Jesper Wengel, PhD^c,
Sónia Silva, PhD^{a,d,*}

^aLIBRO–Laboratório de Investigação em Biofilmes Rosário Oliveira, CEB–Centre of Biological Engineering, University of Minho, Braga, Portugal

^biBB–Institute for Bioengineering and Biosciences, Instituto Superior Técnico, Lisbon University, Lisbon, Portugal

^cBiomolecular Nanoscale Engineering Center, Department of Physics, Chemistry and Pharmacy, University of Southern Denmark, Odense M, Denmark

^dNational Institute for Agrarian and Veterinary Research, Vairão, Vila do Conde, Portugal

Revised 21 July 2021

Abstract

Whereas locked nucleic acid (LNA) has been extensively used to control gene expression, it has never been exploited to control *Candida* virulence genes. Thus, the main goal of this work was to compare the efficacy of five different LNA-based antisense oligonucleotides (ASO) with respect to the ability to control *EFG1* gene expression, to modulate filamentation and to reduce *C. albicans* virulence. *In vitro*, all LNA-ASOs were able to significantly reduce *C. albicans* filamentation and to control *EFG1* gene expression. Using the *in vivo* *Galleria mellonella* model, important differences among the five LNA-ASOs were revealed in terms of *C. albicans* virulence reduction. The inclusion of PS-linkage and palmitoyl-2'-amino-LNA chemical modification in these five LNA gapmers proved to be the most promising combination, increasing the survival of *G. mellonella* by 40%. Our work confirms that LNA-ASOs are useful tools for research and therapeutic development in the candidiasis field.

© 2021 The Author(s). Published by Elsevier Inc. This is an open access article under the CC BY license (<http://creativecommons.org/licenses/by/4.0/>).

Key words: Antisense oligonucleotides; Locked nucleic acid; Candidiasis; Filamentation; *Galleria mellonella*

The antisense technology uses antisense oligonucleotides (ASOs) to target a specific gene involved in diseases by means of RNA-targeting, which can lead to inhibition of gene expression and thus to a blockage in the transfer of genetic information from DNA to protein.¹ ASOs are short oligonucleotides designed to bind target RNA through standard Watson–Crick base pairing.¹ ASOs are often chemically modified in order to protect them against the action of nucleases, thus improving its biodistribution, RNA-affinity and potency.² The phosphorothioate (PS) backbone was one of the early developed chemical modifications, and it is characterized by the substitution of one of the non-bridging phosphate oxygen atoms by a sulfur atom (Figure S1).^{1,3,4} The locked nucleic acid (LNA) is a sugar modification

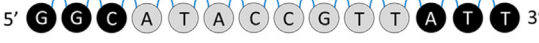
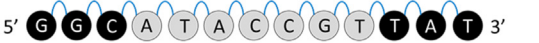
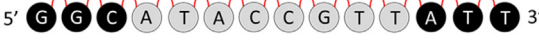
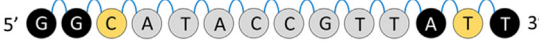


having, relative to native RNA, a methylene bridge between the 2'-oxygen and 4'-carbon atoms of the ribose sugar (Figure S1).^{5,6} A derivative of LNA, named palmitoyl-2'-amino-LNA resulting from the inclusion of an N-palmitoylated nitrogen atom in the 2'-position of the ribose ring, has been developed^{7,8} and shown to display similarly high-affinity binding as LNA to complementary RNA and DNA (Figure S1).^{2,7,9}



Candidiasis is the primary fungal infection, with a mortality rate of about 40%¹⁰ and high costs associated in hospitalized patients.^{10,11} *Candida albicans* remains the most prevalent of all *Candida* species in the world, with a range of incidence of approximately 50%.¹⁰ *C. albicans* pathogenicity is attributed to certain virulence factors, such as its ability to switch from yeast

* Corresponding author at: LIBRO–Laboratório de Investigação em Biofilmes Rosário Oliveira, CEB–Centre of Biological Engineering, University of Minho, 4710-057 Braga, Portugal.

E-mail addresses: soniasilva@deb.uminho.pt sonia.silva@iniav.pt (S. Silva).

Table 1
Sequence of anti-*EFG1* LNA-gapmer ASOs, with the respective length.

ASO	Sequence	PO or	Length	% of GC
		PS	N° of mers	
LNA-gapmer1	5'  3'	PO	14	42.9
LNA-gapmer2	5'  3'	PO	13	46.2
LNA-gapmer3	5'  3'	PS	14	42.9
LNA-gapmer4	5'  3'	PO	14	42.9
LNA-gapmer5	5'  3'	PS	14	42.9
LNA-scrambled	5'  3'	PS	14	43.9

to filamentous forms.^{12–15} In addition, *EFG1* is an important regulator gene of *C. albicans* filamentation,^{16–19} and we recently proved that it is an important target to control *C. albicans* filamentation.²⁰ As a consequence of the rising levels of *C. albicans* resistance to the traditional antifungal therapies (e.g. fluconazole),^{13,21} new alternative therapies, with novel mechanisms of action, enhanced therapeutic potential, improved pharmacokinetics, and lower toxicity, are urgently needed to reach the marketplace to control *C. albicans* infections. Despite the use of nucleic acid mimics to detect *Candida* species,^{22–24} the application of ASOs to treat *Candida* infections is still scarce and it is limited to the first (PS)²⁵ and the second (2'OMe)²⁰ generation of ASOs.

Thus, the main goal of this work was to evaluate the ability of a set of LNA-ASOs, in the so-called gapmer constitution, to control *EFG1* gene expression and to reduce *C. albicans* filamentation (*in vitro*). The ability of the LNA-ASOs to control *C. albicans* virulence in an *in vivo* model (*G. mellonella*) was also assessed.

Methods

Design and synthesis of anti-*EFG1* LNA-gapmers

Five LNA-gapmers were designed against the *C. albicans* *EFG1* (gene orf19.610) target using the sequence 5'-AATAACGGTATGCC-3' as starting point²⁰ for the inclusion of LNA nucleotide modifications. LNA-gapmer1 was used as the standard ASO during this study, and four additional LNA-gapmers were subsequently designed by shortening the central DNA-nucleotide gap (LNA-gapmer2), adding PS-linkages (LNA-gapmer3 and LNA-gapmer5), and adding a palmitoyl-2'-amino-LNA modification (LNA-gapmer4 and LNA-gapmer5) (Table 1). In all LNA-gapmer designs, three LNA nucleotides were introduced consecutively at both 3' and 5'

ends to increase the ASOs stability. Furthermore, in order to ensure compatibility with RNase H-mediated cleavage of the target RNA upon binding, the central regions (gap) were constituted of DNA nucleotides.²⁶ Finally, a scrambled PS LNA-gapmer control was synthesized with three mismatches within the gap (Table 1).

The LNA-gapmers were synthesized using the standard phosphoramidite method on an automated nucleic acid synthesizer (PerSpective Biosystems Expedite 8909 instrument). All standard oligonucleotides were purchased from *Integrated DNA Technologies* (Leuven, Belgium). LNA phosphoramidites were purchased from Qiagen, and the synthesis was performed in 1.0 μmol scale using an LNA T 40 custom primer support (GE Healthcare). LNA phosphoramidites were incorporated according to the following conditions: trichloroacetic acid in CH₂Cl₂ as detritylation reagent; 0.25 M 4,5-dicyanoimidazole (DCI) in CH₃CN as an activator; acetic anhydride in THF (9:91; v/v) as capA solution; N-methylimidazole in THF (1:9; v/v) as capB solution; and a thiolation solution containing 0.2 M phenylacetyl disulfide (PADS) in 3-picoline/CH₃CN (1:1, v/v) for 180 s. The coupling yields were based on the absorbance of the dimethoxytrityl cation (DMT⁺) released after each coupling step. Palmitoyl-2'-amino-LNA phosphoramidite monomer was incorporated by manual-coupling⁷ using 5-[3,5-bis(trifluoromethyl)phenyl]-*H*-tetrazole (0.25 M, in anhydrous acetonitrile) as an activator and extended coupling time (20 min). After the synthesis process, the LNA-gapmers were cleaved from the solid support and the protecting groups removed by treatment with a 1:1 mixture (v/v) of 98% aqueous methanol (v/v) and a 7 M solution of ammonia in methanol for 2 h at room temperature followed by treatment with 32% aqueous ammonia (w/w) at 55 °C for 12 h. The ASOs were characterized by ion-exchange HPLC (IE-HPLC, Lachrom) (Figure S2) and matrix-assisted laser desorption ionization time-to-flight mass spectrometry (MALDI-TOF, Microflex LT, Bruker, Daltonics) (Figure S3).

The purified ASOs were detritylated by treatment with an 80% (w/w) aqueous solution of acetic acid for 20 min at room temperature, precipitated by the addition of ice-cold acetone, and characterized by IE-HPLC (purity >90%) and MALDI-TOF mass spectrometry (confirmation of composition).

Characterization of anti-EFG1 LNA-gapmers

Melting temperatures (T_m values)

The T_m values determined for duplexes involving RNA complementary strands were measured on a PerkinElmer Lambda 35 UV/VIS spectrometer equipment with Peltier Temperature Programmer (PTP6). The concentration of each oligonucleotide was determined optically at 260 nm using their molar extinction coefficients (134,000 L per $M^{-1} cm^{-1}$ of strands). All measurements were performed in medium salt buffer with 220 mM Na^+ (composition: 200 mM NaCl, 20 mM NaH_2PO_4 and 0.1 mM EDTA, pH 7.0). The LNA-gapmer ASOs were mixed with the corresponding unmodified complementary strand at a 1:1 ratio (2.5 nmol of each strand). All melting curves for duplex denaturation were collected at a 260 nm wavelength as a function of temperature in the range from 8 to 80 °C (heating rate of 1 °C per min) (Figure S4). The values of T_m were determined as an average of two individual measurements.

Secondary structure

The secondary structure of the LNA-gapmers was determined by circular dichroism (CD) studies. The spectra were recovered on a JASCO DC 1500 spectrophotometer using cuvettes with 0.1 cm path length and averaged over three scans (320-200 nm, 50 nm min^{-1} intervals, 1 nm bandwidth, and 1 s response time) and with a background corrected using the buffer applied (5 mM $MgCl_2$, 10 mM NaCl and 1 mM sodium phosphate). The LNA-gapmer ASOs were used in the following constitution, *i.e.*, 50 μM RNA, 5 mM $MgCl_2$, 10 mM NaCl, and 1 mM sodium phosphate-pH 7.2. All other strands were prepared using 25 μM of each RNA using the same buffer. Hybridization step was performed by heating to 90 °C for 5 min followed by slow cooling to room temperature followed by spectral recording.

Anti-EFG1 LNA-gapmers cytotoxicity

The cytotoxicity of the LNA-gapmers was determined using a 3T3 cell line (Fibroblasts, Embryonic tissue, Mouse from CCL3, American Type Culture Collection) according to the ISO10993:5.²⁷ For that, 3T3 cells were grown in Dulbecco's Modified Eagle's Medium (DMEM, Biochrom, Germain) supplied by 10% of fetal bovine serum (FBS, Sigma Aldrich) and 1% of antibiotic-containing penicillin and streptomycin (P/S) (Biochrom, Germain). After detachment, a suspension with 1×10^5 cells ml^{-1} was added to a 96-well plate and cells were allowed to grow until attaining 80% confluence. Different concentrations of each LNA-gapmer (10, 40 and 100 nM) were prepared in DMEM medium and 50 μL of each concentration was added to each well. The positive control was prepared by adding 50 μL of DMEM medium and the negative control by adding 50 μL of DMSO to the cells. The plates were incubated for 24 h at 37 °C and 5% CO_2 .

After the incubation period, 10 μL of a solution of 3-(4,5-dimethylthiazol-2-yl)-5-(3-carboxymethoxyphenyl)-2-(4-sulfo-

phenyl)-2H-tetrazolium (MTS, CellTiter 96® Aqueous One Solution Cell Proliferation Assay, Promega) and 1% of D-MEM without phenol was added to each well, and the resulting mixture was incubated for 1 h at 37 °C. The absorbance for each well was measured at 490 nm in a microplate reader (Biochrom EZ Reader 800 Plus, Cambridge, England).

Anti-EFG1 LNA-gapmers performance in vitro

Microorganisms and growth conditions

The *Candida* strain used in this study was *C. albicans* SC5314, a *Candida* collection reference strain from the Biofilm group of the Centre of Biological Engineering (Braga, Portugal). The strain identification was confirmed using a chromogenic medium, CHROMagar™ *Candida*, through the distinction of colony colors and PCR-based sequencing with primers for TS1 and ITS4.²⁸

For all experiments, the yeast strain was subcultured on Sabouraud dextrose agar (SDA; Merck, Germany) and incubated for 24 h at 37 °C. Cells were then inoculated in Sabouraud dextrose broth (SDB; Merck, Germany) and incubated overnight at 37 °C, 120 rpm. After incubation, the cells' suspensions were centrifuged for 10 min, at 3000 $\times g$ and 4 °C, and washed twice with phosphate-buffered saline solution (PBS; pH 7, 0.1 M). Pellets were suspended in 5 ml of Roswell Park Memorial Institute 1640 medium (RPMI; pH 7; Sigma, St Louis, USA), and the cellular density was adjusted for each experiment using a Neubauer chamber (Marienfeld, Land-Konicshofem, Germany) to 1×10^6 cells ml^{-1} . All experiments were performed in triplicate, and at least three independent assays were run.

Effect on filamentation

To evaluate the effect of the LNA-gapmers on *C. albicans* filamentation, yeast cells were incubated with each ASO for 24 h in an Erlenmeyer flask. For that, 5 mL of each LNA-gapmer at 40 nM (prepared on RPMI) was added to 5 mL of *C. albicans* suspension at 1×10^6 cells ml^{-1} (prepared on RPMI). The suspensions were incubated at 37 °C under gentle agitation (120 rpm). The positive control was prepared with 10 mL of the same yeast cell concentration on RPMI. In addition, the LNA-scrambled gapmer was also incubated with *C. albicans* for 24 h (as negative control). After 24 h, aliquots were recovered, and filaments were counted using a Neubauer chamber. The results were presented as percentage (%) of filamentation reduction through the following formula:

%filamentation inhibition

$$= \frac{(\% \text{filamented cells on control} - \% \text{filamented cells on treated sample})}{\% \text{filamented cells on control}}$$

In parallel, the levels of filamentation and the length of the filaments were confirmed through fluorescence microscopy (Olympus BX51) coupled with a DP71 digital camera and the filter used was DAPI 360-370/420 (Olympus Portugal SA, Porto, Portugal). *C. albicans* cells were stained with 1% (v/v) of calcofluor (Sigma-Aldrich, St. Louis, MO, USA) for 15 min in dark conditions, centrifuged for 5 min, and washed twice with ultra-pure water. Images were acquired with the program FluoView FV100 (Olympus). The filaments' length was

determined using ImageJ plug-in software (Maryland, USA) software.

Effect on *EFG1* gene expression

Reverse transcription-qPCR (qRT-PCR) was used to determine the effect of LNA-gapmers on *EFG1* gene expression. After 24 h of incubation, 1 mL of each suspension was collected, subjected to centrifugation for 5 min at 6000 \times g and 4 °C, and then washed once with PBS. RNA extraction was performed using the PureLink RNA Mini Kit (Invitrogen, Carlsbad, CA, USA).²⁰ To avoid potential DNA contamination, samples were treated with DNase I (Deoxyribonuclease I, Amplification Grade, Invitrogen) and the RNA concentration was determined by optical density measurement (NanoDrop 1000 Spectrophotometer Thermo Scientific®). The complementary DNA (cDNA) was synthesized using the Xpert cDNA Synthesis Mastermix (Grisp, Porto, Portugal) in accordance with the manufacturer's instructions, and qRT-PCR (CFX96, Biorad) was performed on a 96-well microtiter plate using Eva Green Supermix (Biorad, Berkeley, USA). Each reaction was performed in triplicate and mean values of relative expression were determined by the $2^{-\Delta\Delta Cq}$ method. The expression of the *EFG1* gene was normalized using the *ACT1 Candida* reference gene.²⁹ Non-transcriptase reverse (NRT) controls were included in each run. The primers were designed using the Primer 3 web-based (Table S1).

Anti-*EFG1* LNA-gapmers performance in vivo

The *Galleria mellonella* caterpillar infection model was used for the *in vivo* studies as previously described by Mil-Homens et al.^{30,31} *G. mellonella* larvae were reared on a pollen grain and bee wax diet at 25 °C in the darkness, and a micro syringe was adapted into a micrometer range so as to control the injection volume into hemolymph of larvae.

Toxicity evaluation

To test toxicity of the anti-*EFG1* LNA-gapmers *in vivo*, 10 *G. mellonella* larvae were injected, *via* the hindmost left proleg previously sanitized with 70% (v/v) ethanol, with 5 μ L of two distinct concentrations (40 and 100 nM both prepared with PBS) of each LNA-gapmer. As control, a set of larvae was injected with the same volume of PBS. Larvae were placed in Petri dishes and stored in the dark at 37 °C. Larvae survival was recorded over 4 days, and survival curves were constructed.

Galleria mellonella survival

To study the effect of the LNA-gapmers on *G. mellonella* survival rate, larvae were injected with *C. albicans* and each LNA-gapmer. The concentration of *C. albicans* to be injected (7×10^7 cells mL⁻¹) was selected on the basis of the *G. mellonella* lethality results after injection with different concentrations of yeast cells (between 7×10^7 cells mL⁻¹ and 2×10^8 cells mL⁻¹) (data not shown). Next, 10 larvae were injected with 5 μ L of a suspension of *C. albicans* at 7×10^7 cells mL⁻¹ mixed with 40 nM of each LNA-gapmer. Larvae were placed in Petri dishes and stored in the dark at 37 °C for 3 days, whereupon survival curves were constructed. Caterpillars were considered dead when they displayed no movement in response to a touch with tweezers.

Histological analysis of *G. mellonella* fat bodies was also performed to evaluate the effects of LNA-gapmers on *C.*

albicans filamentation. For each condition, two larvae were recovered after pre-determined times (24 h and 48 h) and their fat bodies were removed through an incision in the midline of the ventral with a scalpel blade. The fat bodies were stored in 4% (v/v) paraformaldehyde at 4 °C to prepare for histological processing. The tissue was mounted in paraffin blocks and cut in sections of 4–5 μ m, which were stained with hematoxylin–eosin (HE) and periodic acid Schiff (PAS).^{32,33} The yeast and hyphae of *C. albicans* were observed under a light microscope. For analysis of filamentation, all areas of the histological section stained with PAS that contained hyphae and yeast cells were photographed with an OLYMPUS BX51 microscope coupled with a DP71 digital camera (Olympus Portugal SA, Porto, Portugal).

Statistical analysis

Data are expressed as the mean \pm standard deviation (SD) of a least three independent experiments. Results were compared using two-way analysis of variance (ANOVA). All tests were performed with a confidence level of 95%. Kaplan–Meier survival curves were plotted and differences in survival were calculated by using log-rank Mantel–Cox statistical test. All performed with GraphPad Prism 6® (CA, USA).

Results

Characterization of anti-*EFG1* LNA-gapmers

Figure 1 represents the results of the secondary structure for single-stranded (ss) and double-stranded(ds)-LNA:RNA compounds. All duplexes presented a similar overall conformation, thus indicating no major alterations in secondary structure. For single-strands, all LNA-gapmers present bands as expected from literature observations,^{34,35} *i.e.* low positive bands around 270 nm and 220 nm and low negative bands around 240 nm and 210 nm. The dsRNA, defined as A-duplex, is characterized by a strong positive band at 270 nm coupled with a strong negative band at 210 nm,^{34,36,37} as it can be seen for dsLNA:RNA in all LNA-gapmers.

Table 2 and Figure S4 show the values of T_m measured for all LNA-gapmers with RNA complement. The LNA-gapmer1 presented a T_m of 70 °C and similarly, the LNA-gapmer2 (exclusion of one nt) presented a T_m of 72 °C. In contrast, LNA-gapmer3 (addition of PS-linkages), LNA-gapmer4 (addition of the palmitoyl-2'-amino-LNA modification) and LNA-gapmer5 (addition of PS-linkages and the palmitoyl-2'-amino-LNA modification) showed a significant decrease in T_m for 63 °C, 65 °C and 56 °C, respectively.

Cytotoxicity of anti-*EFG1* LNA-gapmers

The *in vitro* cytotoxicity was assessed on 3T3 cells and using different concentrations of LNA-gapmers (10, 40 and 100 nM) (Figure 2). These results show that all LNA-gapmers are non-cytotoxic in concentrations up to 40 nM, as the relative 3T3 cells viability was >70% under these conditions.²⁷

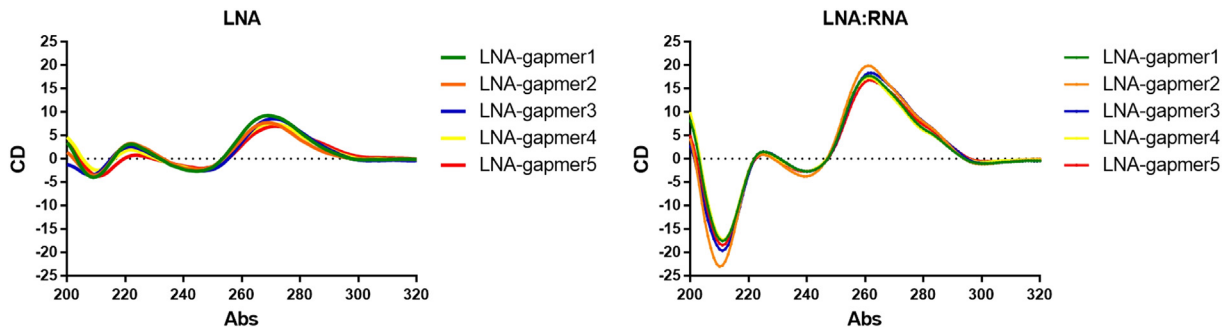


Figure 1. Studies of characterization of anti-*EFG1* LNA-gapmer ASOs. Evaluation of the secondary ASOs structure by circular dichroism spectral analysis of single-strands (ssLNA) and double-stranded complexes (dsLNA:RNA; dsLNA:DNA). The spectra were recorded in a 0.1 cm path length cuvette. Each spectrum was recorded from the averaged over three scans (320–200 nm, 50 nm min⁻¹ intervals, 1 nm bandwidth, and 1 s response time).

Table 2

Characterization of anti-*EFG1* LNA-gapmer ASOs. The thermal denaturation temperatures (T_m values, °C) of the LNA-gapmer ASOs were determined in medium salt buffer against its RNA complement. All melting curves were collected at a 260 nm wavelength as a function of temperature in the range from 8 to 80 °C (heating rate of 1 °C per min).

LNA-gapmer	Melting temperatures (T_m , °C) Medium salt buffer
LNA-gapmer1	70.2
LNA-gapmer2	71.6
LNA-gapmer3	63.2
LNA-gapmer4	65.2
LNA-gapmer5	55.7

Anti-*EFG1* LNA-gapmer ASO performance *in vitro*

Based on the cytotoxicity results, the ASO concentration of 40 nM was selected for the *in vitro* experiments. The effect of all LNA-gapmers on *C. albicans* filamentation and on the *EFG1* gene expression was evaluated after 24 h of treatment. To note, the *C. albicans* strain used under this study presents a high

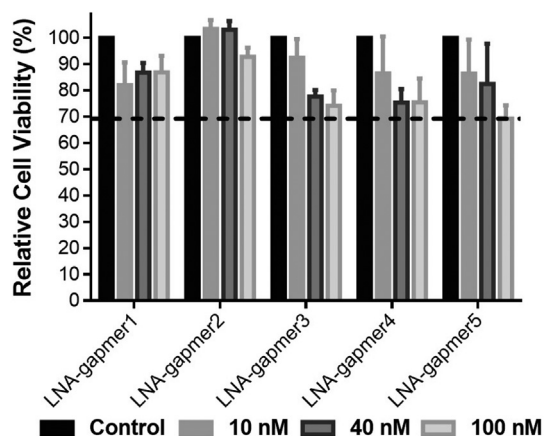


Figure 2. Studies of cytotoxicity of anti-*EFG1* LNA-gapmer ASOs. Relative cell viability (%) determined by the absorbance (Abs (490 nm) cm⁻²) of formazan product obtained from 3T3 cell line, treated with different concentrations of LNA-gapmers (10, 40, 100 nM). The control is compared to cells without ASO treatment.

filamentation capacity (Figure S5, A) together with high levels of *EFG1* gene expression (Figure S5, B). Figure 3, A shows that all LNA-gapmers were able to control *C. albicans* filamentation with values of inhibition greater than 40%. The LNA-gapmer1 was capable to reduce around 45% of *C. albicans* filamentation, and this reduction increased for all other LNA-gapmers, however without statistically significant differences (P value > 0.05). The LNA-gapmer2 was able to reduce into 50% *C. albicans* filamentation and the LNA-gapmer3–5 into 55% (Figure 3, A). The results revealed that the LNA-gapmers modified with PS-linkages and the palmitoyl-2'-amino-LNA display a similar *in vitro* performance. To note, the LNA-scrambled ASO tested was unable to reduce *C. albicans* filamentation (Figure S6).

Figure 3, B shows that all LNA-gapmers were able to reduce the levels of *EFG1* gene expression with values also greater than 40%. LNA-gapmer1 was able to reduce the levels of *EFG1* expression by approximately 74%. Moreover, the LNA-gapmer2 and LNA-gapmer3 had a similar performance to LNA-gapmer1, with reductions of approximately 78% and 71%, respectively. Concerning the LNA-gapmer4 and LNA-gapmer5, the levels of gene inhibition were slightly reduced, reaching around 44% and 61%, respectively. It is important to note that the results were statistically significant when comparing the performance of all LNA-gapmers with the untreated cells (P value < 0.05), despite not presenting statistically significant differences among the LNA-gapmers (P value > 0.05).

The epifluorescence microscopy images (Figure 3, C) corroborate the results in the number of *C. albicans*' filaments decrease (Figure 3, A), also demonstrating its ability to reduce the filament length. Concerning this issue, the highest impact was observed with the LNA-gapmer3 and LNA-gapmer5, achieving values of reduction of around 65% and 56%, respectively.

Anti-*EFG1* LNA-gapmers performance *in vivo*

The *in vivo* effects of the anti-*EFG1* LNA-gapmer ASOs were evaluated using the *G. mellonella* model³⁸ (Figure 4). Notably, experiments showed the absence of *in vivo* toxicity for all the LNA-gapmers (40 nM) (Figure 4, A).

To evaluate the performance of the LNA-gapmers *in vivo*, *G. mellonella* larvae were injected with a lethal dose of *C. albicans* (7×10^7 cells/mL) together with 40 nM of each LNA-gapmer. As

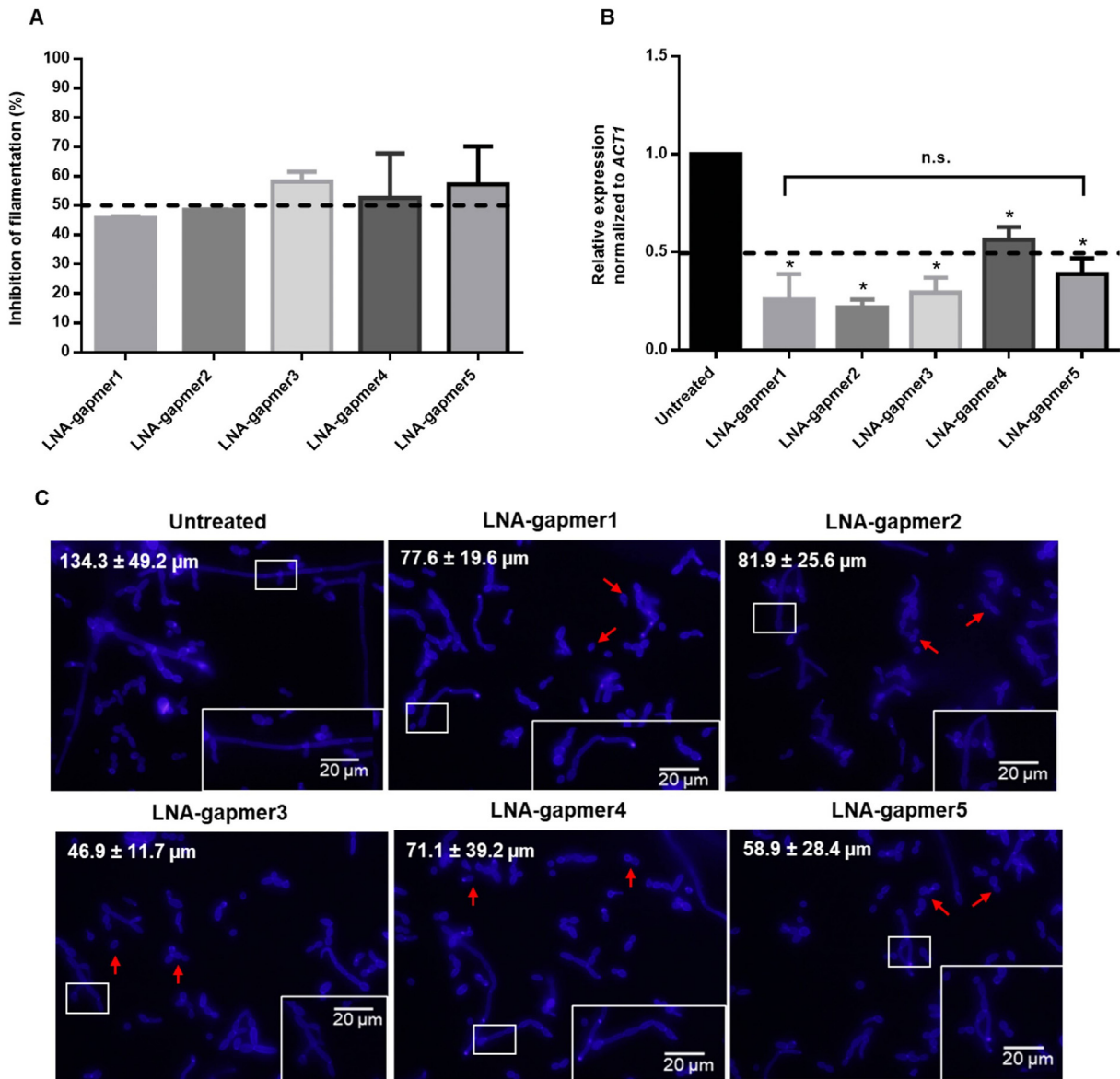


Figure 3. Performance of anti-*EFG1* LNA-gapmer ASOs *in vitro*. Effect of treatment of *C. albicans* with LNA-gapmers (40 nM) during 24 h. (A) Percentage of *C. albicans* filamentation reduction determined by microscopic observation. As control, the *C. albicans* cells were prepared only in RPMI (without ASOs). (B) Levels of *EFG1* gene expression evaluated by qRT-PCR. Untreated represents an experiment prepared only with cells on RPMI (without ASOs). (C) Epifluorescence microscopy image analysis of *C. albicans* cells stained with calcofluor. The number in each image refers to the average length of filaments. The arrows highlight the *C. albicans* in yeast morphology. Error bars represent standard deviation. *Significant differences between the untreated cells and the LNA-gapmers tested ($P < 0.05$).

illustrated in Figure 4, B, from the set of larvae injected with *C. albicans* cells (control) only 57% at 24 h, 33% at 48 h and 20% at 72 h of larvae were alive. It is important to underline that the treatment with all LNA-gapmers increased the *G. mellonella* survival rate. The larvae injection with the LNA-gapmer1 and LNA-gapmer2 increased the survival, respectively, to 80% and 67% at 24 h and to 53% and 47% at 48 h, with no effect observed at 72 h (with 20% of survival in control and with both LNA-gapmers). The treatment of larvae with the LNA-gapmer3 and LNA-gapmer4 displayed an increase in the survival rate of approximately 90% and 83% at 24 h, 60% at 48 h and 30% and 33% at 72 h, respectively. The most promising of all LNA-

gapmers was the LNA-gapmer5, which induced a survival rate of around 93% at 24 h, 77% at 48 h and 60% at 72 h.

In parallel, the fat body of larvae (Figure S7) was recovered and processed for histological analysis (Figure 4, C). As illustrated, yeast's cells are organized into clusters located around the organs or scattered around the adipose tissue. Sections of larvae infected only with *C. albicans* (control) showed intense *C. albicans* clusters composed mostly of filamentous forms, with a significant increase in tissue area engaged by hyphae from 24 h to 48 h post infection. Larvae sections treated with LNA-gapmer4 and LNA-gapmer5 revealed a notable decrease in the number of *C. albicans* as filamentous

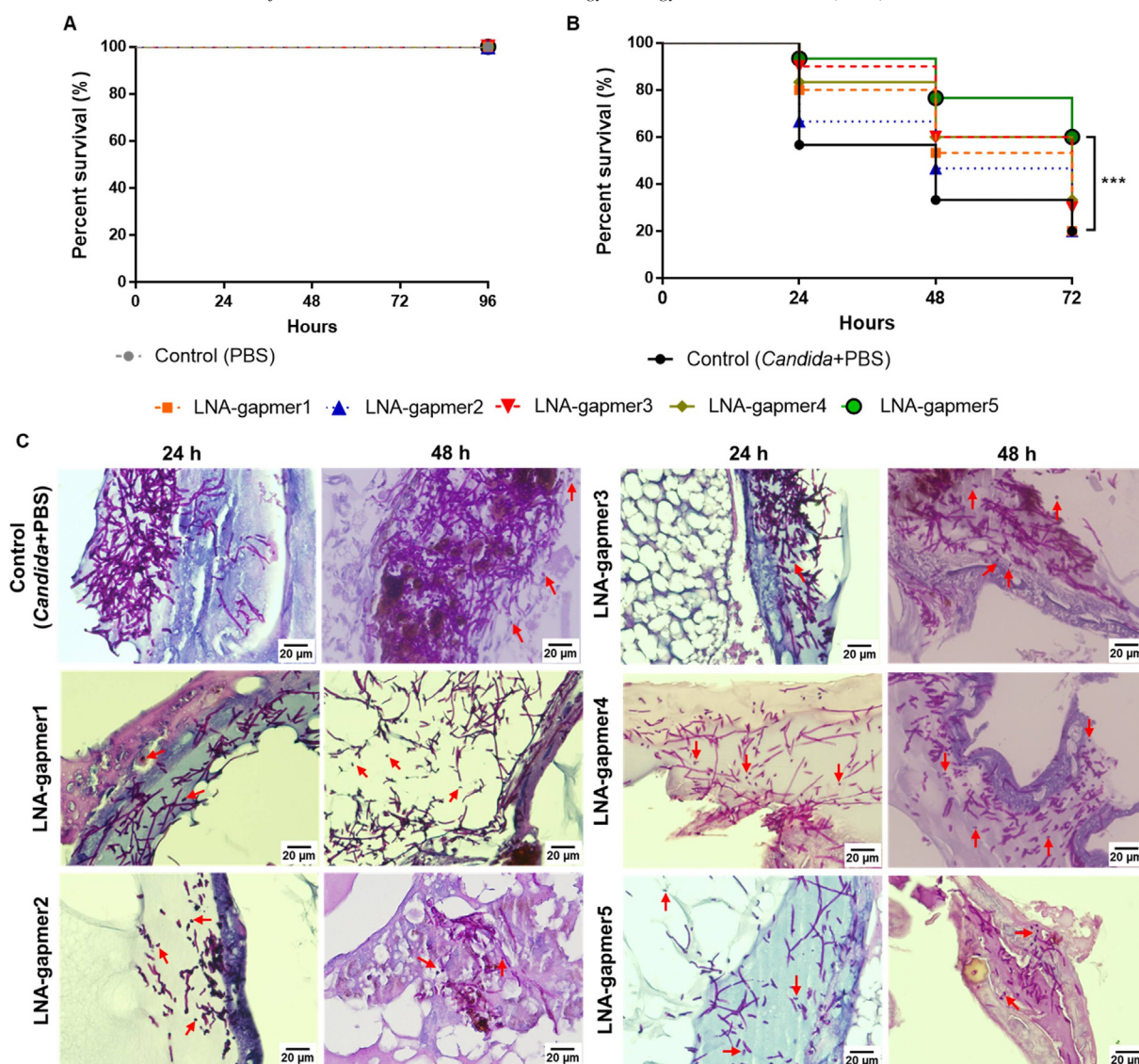


Figure 4. Performance of anti-*EFG1* LNA-gapmer ASOs *in vivo*. (A) Anti-*EFG1* LNA-gapmers toxicity evaluation after injection of *G. mellonella* larvae with 40 nM of each ASO during 96 h. As control larvae were injected only with PBS. (B) Survival curves of *G. mellonella* larvae infected with *C. albicans* SC5314 (7×10^7 cells mL⁻¹ injected per larva) and treated with each LNA-gapmer (40 nM) during 72 h. Larvae were infected with a single dose of each LNA-gapmer at the same time of *C. albicans* cells and as control infected larvae were only injected with PBS. (C) Histological sections of the fat bodies of *G. mellonella* infected with *C. albicans* and treated with each LNA-gapmer (40 nM) at 24 h and 48 h. The tissues of larvae were stained with PAS coloration. The arrows highlight the *C. albicans* in yeast morphology. The magnification was 400x. Results represent means of three independent assays for 10 larvae per treatment. ***Significant difference between the control (*Candida* + PBS) and the LNA-gapmer5 (P value < 0.001).

and consequently led to a significant reduction in the area of fat body invaded by *C. albicans*.

Discussion

In the last decade, the number of successful applications of ASOs for the treatment of human diseases^{39–46} and to manage virus and bacterial infections^{47–49} has increased. However, the ASO technology has been poorly exploited to control *Candida* virulence determinants, and to date there are no reports of applications of LNA chemical modification to control *Candida* virulence determinants. Through this work, the efficacy of LNA-gapmer ASOs, designed to hybridize specifically to an *EFG1*

target, was compared, concerning its ability to control *EFG1* gene expression and to reduce *C. albicans* filamentation, in order to control *in vivo* *C. albicans* virulence. Therefore, a set of five LNA-gapmers was designed with different lengths and different chemical modifications, such as the PS-linkages or/and the palmitoyl-2'-amino-LNA chemical modification/s.

Initially, it was important to confirm the composition and the purity of all LNA-gapmers (Figures S2 and S3) and to verify if the inclusion of LNA chemical modifications to the sequence influences its secondary structure (Figure 1) and its hybridization stability (Table 2). In many aspects the LNA gapmer ASOs behaved quite similarly. However, the inclusion of PS-linkages (LNA-gapmer3) led to a decrease in duplex thermal denaturation

temperature (T_m value) against RNA complement. As described in the literature,^{50,51} the inclusion of the PS modification and the palmitoyl-2'-amino-LNA (LNA-gapmer4 and LNA-gapmer5) also reduced the thermal denaturation temperature of the corresponding duplexes when compared to the thermal denaturation temperatures of the duplexes involving the reference LNA-gapmer1. Of all LNA-gapmers characterized, LNA-gapmer5 displayed the lowest affinity. The decrease in thermal denaturation temperature upon incorporation of the palmitoyl-2'-amino-LNA monomers corresponds with results reported earlier.⁸

The *in vitro* and *in vivo* efficacy of each LNA-gapmer was evaluated at 40 nM since none of them presented *in vitro* (Figure 2) or *in vivo* toxicity (Figure 4, A). The *in vitro* results demonstrate the capacity of the LNA-gapmers to control *EFG1* gene expression by 40%-60% (Figure 3, B) and *C. albicans'* filamentation around 50% (Figure 3, A), as well as the filaments length on 60% (Figure 3, C). The inclusion of PS-linkages (LNA-gapmer3) enhanced filamentation reduction, however, without any additional effect on *EFG1* gene silencing. On the other hand, the inclusion of palmitoyl-2'-amino-LNA monomers on LNA-gapmer4 and LNA-gapmer5 did not significantly enhance the filamentation control or the gene silencing when compared to the performance of the other LNA-gapmers. It should be pointed out that the ability of LNA-gapmer ASOs to control *C. albicans'* filamentation and to reduce the filaments' length is crucial to reduce *C. albicans* pathogenicity, once it decreases *C. albicans'* ability to invade the human body tissues and to escape of host's immune system.⁵²⁻⁵⁴

The *G. mellonella* caterpillar infection model was used to evaluate the effects of the LNA-gapmer ASOs on *C. albicans* virulence (Figure 4). Interestingly, in contrast to the *in vitro* experiments, *in vivo* results highlight pronounced differences among the individual LNA-gapmers. Thus, although the LNA-gapmer5 did not show the best performance *in vitro* (Figure 3), this gapmer was the most efficient with respect to the control of *in vivo C. albicans'* virulence (Figure 4, B and C). In fact, larvae treated with LNA-gapmer5 significantly increased *G. mellonella* survival from 20% to 60% (at 72 h of treatment). The histological images corroborated these findings with a notable reduction in the number of *C. albicans* filamentous cells and a consequent reduction in area of *G. mellonella* invasion (Figure 4, C).

This work revealed that it is possible to design nucleic acid mimics to control important virulence factors behind the *Candida* infections. The application of LNA-gapmer ASO confirms the possibility to control virulence determinants of *C. albicans* and thus to control its pathogenicity. Moreover, the LNA-type gapmer ASOs modifications with PS-linkages and palmitoyl-2'-amino-LNA monomers are favorable for *in vivo* performance and constitute promising lead structures for development of drugs against *Candida* species.

However, considering any possible future clinical applications in the control of local candidiasis (oral, vaginal, and urinary), as well as of systemic infections (blood), additional studies are imperative. It will be necessary to investigate strategies for LNA-gapmer ASO delivery and to extend the *in vivo* studies for a more complex and robust model, as a mouse model.

Credit Author Statement

Daniela Araújo, Sónia Silva, Per Trolle Jørgensen and Jesper Wengel conceived and designed the study. Daniela Araujo, Dalila Mil-Homens and Maria Elisa Rodrigues conducted the experiments. Daniela Araujo and Sónia Silva wrote the manuscript. Mariana Henriques, Sónia Silva and Jesper Wengel performed the analysis and read the paper. All authors read and approved the manuscript.

Acknowledgments

This study was supported by the Portuguese Foundation for Science and Technology (FCT) under the strategic funding of UIDB/04469/2020 unit and BioTecNorte operation (NORTE-01-0145-FEDER-000004) funded by the European Regional Development Fund under the scope of Norte2020-Programa Operacional Regional do Norte and Daniela Eira Araújo [SFRH/BD/121417/2016] PhD grant. The authors also acknowledge the project funding by the "02/SAICT/2017-Projetos de Investigação Científica e Desenvolvimento Tecnológico (IC&DT)-POCI-01-0145-FEDER-028893". VILLUM Fonden is acknowledged for funding the Biomolecular Nano-scale Engineering Center (BioNEC), a Villum center of excellence, grant number VKR18333. Funding received by iBB-Institute for Bioengineering and Biosciences from FCT (UID/BIO/04565/2020) and Programa Operacional Regional de Lisboa 2020 (Project No. 007317) is also acknowledged. We acknowledge Dr. Lucília Goreti Pinto, Life and Health Sciences Research Institute (ICVS), School of Medicine, University of Minho, for processing and sectioning *G. mellonella* tissue samples.

The authors declare no conflict of interest.

Appendix A. Supplementary data

Supplementary data to this article can be found online at <https://doi.org/10.1016/j.nano.2021.102469>.

References

- Dias N, Stein CA. Antisense oligonucleotides: basic concepts and mechanisms. *Mol Cancer Ther* 2002;**1**(5):347-55.
- Chan JHP, Lim S, Wong WSF. Antisense oligonucleotides: from design to therapeutic application. *Clin Exp Pharmacol Physiol* 2006;**33**:533-40.
- Kurreck J. Antisense technologies: improvement through novel chemical modifications. *Eur J Biochem* 2003;**270**(8):1628-44.
- Khvorova A, Watts JK. The chemical evolution of oligonucleotide therapies of clinical utility. *Nat Biotechnol* 2017;**35**(3):238-48.
- Koshkin AA, Singh SK, Nielsen P, Rajwanshi VK, Kumar R, Meldgaard M, et al. LNA (locked nucleic acids): synthesis of the adenine, cytosine, guanine, 5-methylcytosine, thymine and uracil bicyclonucleoside monomers, oligomerisation, and unprecedented nucleic acid recognition. *Tetrahedron* 1998;**54**(14):3607-30.
- Obika S, Nanbu D, Hari Y, Andoh JI, Morio KI, Doi T, et al. Stability and structural features of the duplexes containing nucleoside analogues with a fixed N-type conformation, 2'-O,4'-C-methylenribonucleosides. *Tetrahedron Lett* 1998;**39**:5401-4.
- Johannsen MW, Crispino L, Wamberg MC, Kalra N, Wengel J. Amino acids attached to 2'-amino-LNA: synthesis and excellent duplex stability. *Org Biomol Chem* 2011;**9**(1):243-52.

8. Ries A, Kumar R, Lou C, Kosbar T, Vengut-Climent E, Jørgensen PT, et al. Synthesis and biophysical investigations of oligonucleotides containing galactose-modified DNA, LNA, and 2'-amino-LNA monomers. *J Org Chem* 2016;**81**(22):10845-56.
9. Fluiter K, Frieden M, Vreijling J, Rosenbohm C, De Wissel MB, Christensen SM, et al. On the *in vitro* and *in vivo* properties of four locked nucleic acid nucleotides incorporated into an anti-H-Ras antisense oligonucleotide. *ChemBiochem* 2005;**6**(6):1104-9.
10. Koehler P, Stecher M, Cornely OA, Koehler D, Vehreschild MJGT, Bohlius J, et al. Morbidity and mortality of candidaemia in Europe: an epidemiologic meta-analysis. *Clin Microbiol Infect* 2019;**25**(10):1200-12.
11. Heimann SM, Cornely OA, Wisplinghoff H, Kochanek M, Stoppel D, Padosch SA, et al. Candidemia in the intensive care unit: analysis of direct treatment costs and clinical outcome in patients treated with echinocandins or fluconazole. *Eur J Clin Microbiol Infect Dis* 2015;**34**(2):331-8.
12. Silva S, Negri M, Henriques M, Oliveira R, Williams DW, Azeredo J. *Candida glabrata*, *Candida parapsilosis* and *Candida tropicalis*: biology, epidemiology, pathogenicity and antifungal resistance. *FEMS Microbiol Rev* 2012;**36**(2):288-305.
13. Silva S, Rodrigues C, Araújo D, Rodrigues M, Henriques M. *Candida* species biofilms' antifungal resistance. *J Fungi* 2017;**3**(1):8.
14. Mayer FL, Wilson D, Hube B. *Candida albicans* pathogenicity mechanisms. *Virulence* 2013;**4**(2):119-28.
15. Araújo D, Henriques M, Silva S. Portrait of *Candida* species biofilm regulatory network genes. *Trends Microbiol* 2017;**1**:62-75.
16. Stoldt VR, Sonneborn A, Leuker CE, Ernst JF. Efg1p, an essential regulator of morphogenesis of the human pathogen *Candida albicans*, is a member of a conserved class of bHLH proteins regulating morphogenetic processes in fungi. *EMBO J* 1997;**16**(8):1982-91.
17. Nobile CJ, Mitchell AP. Regulation of cell-surface genes and biofilm formation by the *C. albicans* transcription factor Bcr1p. *Curr Biol* 2005;**15**(12):1150-5.
18. Nobile CJ, Fox EP, Nett JE, Sorrells TR, Mitrovich QM, Hernday AD, et al. A recently evolved transcriptional network controls biofilm development in *Candida albicans*. *Cell* 2011;**148**:126-38.
19. Connolly L, Riccombeni A, Grózer Z, Holland LM, Lynch DB, Andes DR, et al. The APSES transcription factor Efg1 is a global regulator that controls morphogenesis and biofilm formation in *Candida parapsilosis*. *Mol Microbiol* 2013;**90**:36-53.
20. Araújo D, Azevedo NM, Barbosa A, Almeida C, Rodrigues ME, Henriques M, et al. Application of 2'-OMethylRNA' antisense oligomer to control *Candida albicans* EFG1 virulence determinant. *Mol Ther - Nucleic Acids* 2019;**18**:508-17.
21. Yao D, Chen J, Chen W, Li Z, Hu X. Mechanisms of azole resistance in clinical isolates of *Candida glabrata* from two hospitals in China. *Infect Drug Resist* 2019:771-81.
22. Lischewski A, Amann RI, Harmsen D, Merkert H, Hacker J, Morschhäuser J. Specific detection of *Candida albicans* and *Candida tropicalis* by fluorescent in situ hybridization with an 18S rRNA-targeted oligonucleotide probe. *Microbiology* 1996;**142**(10):2731-40.
23. Hagedorn PH, Yakimov V, Ottosen S, Kammler S, Nielsen NF, Høg AM, et al. Hepatotoxic potential of therapeutic oligonucleotides can be predicted from their sequence and modification pattern. *Nucleic Acid Ther* 2013;**23**(5):302-10.
24. Navarro IB, Nava A. Oligonucleotides of *Candida albicans*, detection method and kit comprising same. WO 2015/060704A1.
25. Testa S, Disney M, Gryaznov S, Turner D. Methods and compositions for inhibition of rna splicing. WO2000055374.
26. DeVos SL, Miller TM. Antisense oligonucleotides : treating neurodegeneration at the level of RNA. *Neurotherapeutics* 2013;**10**:486-97.
27. International Organization for Standardization. *ISO10993-5:2009. Biological evaluation of medical devices. Part 5: tests for in vitro cytotoxicity* Third edition. ; 2009.
28. Williams DW, Wilson MJ, Lewis MAO, John A, Potts C. Identification of *Candida* species by PCR and restriction fragment length polymorphism analysis of intergenic spacer regions of ribosomal DNA. *J Clin Microbiol* 1995;**33**(9):2476-9.
29. Nailis H, Coenye T, Van Nieuwerburgh F, Deforce D, Nelis HJ. Development and evaluation of different normalization strategies for gene expression studies in *Candida albicans* biofilms by real-time PCR. *BMC Mol Biol* 2006;**7**:1-9.
30. Mil-Homens D, Bernardes N, Fialho AM. The antibacterial properties of docosahexaenoic omega-3 fatty acid against the cystic fibrosis multi-resistant pathogen *Burkholderia cenocepacia*. *FEMS Microbiol Lett* 2012;**328**(1):61-9.
31. Mil-Homens D, Ferreira-Dias S, Fialho AM. Fish oils against *Burkholderia* and *Pseudomonas aeruginosa*: *in vitro* efficacy and their therapeutic and prophylactic effects on infected *Galleria mellonella* larvae. *J Appl Microbiol* 2016;**120**(6):1509-19.
32. Churukian CJ, Schenk EA. Rapid Grocott's methenamine silver nitrate method for fungi and pneumocystis carinii. *Am J Clin Pathol* 1977;**68**(3):427-8.
33. Perdoni F, Falleni M, Tosi D, Cirasola D, Romagnoli S, Braidotti P, et al. A histological procedure to study fungal infection in the wax moth *Galleria mellonella*. *Eur J Histochem* 2014;**58**(3):258-62.
34. Chauca-Diaz AM, Choi YJ, Resendiz MJE. Biophysical properties and thermal stability of oligonucleotides of RNA containing 7,8-dihydro-8-hydroxyadenosine. *Biopolymers* 2015;**103**(3):167-74.
35. Szabat M, Gudanis D, Kotkowiak W, Gdaniec Z, Kierzek R, Pasternak A. Thermodynamic features of structural motifs formed by β -L-RNA. *PLoS One* 2016;**11**(2):e0149478.
36. Tsai CS. *Biomacromolecules structure: nucleic acids. Biomacromolecules: introduction to structure, function and informatics*. First Edition. Canada: John Wiley & Sons, Inc; 2007:55-93.
37. Choi Y, Gibala K, Ayele T, Deventer K, Resendiz M. Biophysical properties, thermal stability and functional impact of 8-oxo-7,8-dihydroguanine on oligonucleotides of RNA—a study of duplex, hairpins and the aptamer for preQ1 as models. *Nucleic Acids Res* 2017;**45**(4):2099-111.
38. Junqueira JC. *Galleria mellonella* as a model host for human pathogens. *Virulence* 2012;**3**(6):474-6.
39. Jepsen JS, Sørensen MD, Wengel J. *Locked nucleic acid: a potent nucleic acid analog in therapeutics and biotechnology. Vol. 14, oligonucleotides*. Mary Ann Liebert, Inc; 2004:130-46.
40. Frieden M, Orum H. Locked nucleic acid holds promise in the treatment of cancer. *Curr Pharm Des* 2008;**14**(11):1138-42.
41. Yamamichi N, Shimomura R, Inada K, Sakurai K, Haraguchi T, Ozaki Y, et al. Locked nucleic acid in situ hybridization analysis of miR-21 expression during colorectal cancer development. *Clin Cancer Res* 2009;**15**(12):4009-16.
42. Morinaga S, Nakamura Y, Atsumi Y, Murakawa M, Yamaoku K, Aoyama T, et al. Locked nucleic acid in situ hybridization analysis of microRNA-21 predicts clinical outcome in patients after resection for pancreatic cancer treated with adjuvant gemcitabine monotherapy. *Clin Cancer Res* 2016;**36**(3):1083-8.
43. Torres A, Kozak J, Korolczuk A, Rycak D, Wdowiak P, Maciejewski R, et al. Locked nucleic acid-inhibitor of miR-205 decreases endometrial cancer cells proliferation *in vitro* and *in vivo*. *Oncotarget* 2016;**7**(45):73651-63.
44. Ahmadi S, Sharifi M, Salehi R. Locked nucleic acid inhibits miR-92a-3p in human colorectal cancer, induces apoptosis and inhibits cell proliferation. *Cancer Gene Ther* 2016;**23**(7):199-205.
45. Nedaenia R, Sharifi M, Avan A, Kazemi M, Rafiee L, Ghayour-Mobarhan M, et al. Locked nucleic acid anti-MIR-21 inhibits cell growth and invasive behaviors of a colorectal adenocarcinoma cell line: LNA-anti-MIR as a novel approach. *Cancer Gene Ther* 2016;**23**(8):246-53.
46. Ishige T, Itoga S, Matsushita K. Locked nucleic acid technology for highly sensitive detection of somatic mutations in cancer. *Adv Clin Chem* 2018;**83**:53-72.

47. Deng Y, Nong L, Huang W, Pang G, Wang Y. Inhibition of hepatitis B virus (HBV) replication using antisense LNA targeting to both S and C genes in HBV. *Zhonghua Gan Zang Bing Za Zhi* 2009;**17**:900-4.
48. Warren TK, Whitehouse CA, Wells J, Welch L, Charleston JS, Heald A, et al. Delayed time-to-treatment of an antisense morpholino oligomer is effective against lethal Marburg virus infection in *Cynomolgus macaques*. *PLoS Negl Trop Dis* 2016;**10**(2):1-18.
49. Sully EK, Geller BL. Antisense antimicrobial therapeutics. *Curr Opin Microbiol* 2016;**3**(33):47-55.
50. Crooke ST. Progress in antisense technology. *Annu Rev Med* 2004;**55**: 61-95.
51. Lima JF, Cerqueira L, Figueiredo C, Oliveira C, Azevedo NF, Frias R, et al. Anti-miRNA oligonucleotides: a comprehensive guide for design. *RNA Biol* 2018;**15**(3):338-52.
52. Lo HJ, Köhler JR, Didomenico B, Loebenberg D, Cacciapuoti A, Fink GR. Nonfilamentous *C. albicans* mutants are avirulent. *Cell* 1997;**90**(5): 939-49.
53. Lu Q, Jayatilake JAMS, Samaranayake LP, Jin L. Hyphal invasion of *Candida albicans* inhibits the expression of human β -defensins in experimental oral candidiasis. *J Invest Dermatol* 2006;**126**(9):2049-56.
54. Alves C, Wei X-Q, Silva S, Azeredo J, Henriques M, Williams DW. *Candida albicans* promotes invasion and colonisation of *Candida glabrata* in a reconstituted human vaginal epithelium. *J Infect* 2014;**69** (4):396-407.